microbial biotechnology

Open Access

Structural analysis and biochemical properties of laccase enzymes from two *Pediococcus* species

Isidoro Olmeda,[1,‡] Patricia Casino,[2,3,4,‡] Robert E. Collins,[5,6,‡] Ramón Sendra,[2,‡] Sara Callejón,[1,†] Juanjo Huesa,[2] Alexei S. Soares,[7] Sergi Ferrer[1] and Isabel Pardo[1,8,*]

[1]*ENOLAB, Institut de Biotecnologia i Biomedicina (BioTecMed), Universitat de València, Valencia, Spain.*
[2]*Departament de Bioquímica i Biologia Molecular, Universitat de València, Valencia, Spain.*
[3]*Institut de Biotecnologia i Biomedicina (BioTecMed), Universitat de València, Valencia, Spain.*
[4]*Group 739 of the Centro de Investigación Biomédica en Red sobre Enfermedades Raras (CIBERER) del Instituto de Salud Carlos III, Valencia, Spain.*
[5]*Office of Educational Programs, Brookhaven National Laboratory, Upton, NY 11973, USA.*
[6]*Department of Chemistry and Physical Sciences, Quinnipiac University, Hamden, CT 06518, USA.*
[7]*Photon Sciences Directorate, Brookhaven National Laboratory, Upton, NY 11973, USA.*
[8]*Departament de Microbiologia i Ecologia, Universitat de València, Valencia, Spain.*

Summary

Prokaryotic laccases are emergent biocatalysts. However, they have not been broadly found and characterized in bacterial organisms, especially in lactic acid bacteria. Recently, a prokaryotic laccase from the lactic acid bacterium *Pediococcus acidilactici* 5930, which can degrade biogenic amines, was discovered. Thus, our study aimed to shed light on laccases from lactic acid bacteria focusing on two *Pediococcus* laccases, *P. acidilactici* 5930 and *Pediococcus pentosaceus* 4816, which have provided valuable information on their biochemical activities on redox mediators and biogenic amines. Both laccases are able to oxidize canonical substrates as ABTS, ferrocyanide and 2,6-DMP, and non-conventional substrates as biogenic amines. With ABTS as a substrate, they prefer an acidic environment and show sigmoidal kinetic activity, and are rather thermostable. Moreover, this study has provided the first structural view of two lactic acid bacteria laccases, revealing new structural features not seen before in other well-studied laccases, but which seem characteristic for this group of bacteria. We believe that understanding the role of laccases in lactic acid bacteria will have an impact on their biotechnological applications and provide a framework for the development of engineered lactic acid bacteria with enhanced properties.

Received 25 September, 2020; revised 22 December, 2020; accepted 31 December, 2020.
*For correspondence. E-mail Isabel.Pardo@uv.es; Tel. +34963544390; Fax +34 963544570.
Present address: †ENARTIS Wine Tech, ENARTIS SEPSA S.A.U. Pol, Industrial Alces,Avda de los vinos, 18, Alcázar de San Juan, Ciudad Real, 13600, Spain.
‡These authors have equally contributed to the work.
Microbial Biotechnology (2021) **14**(3), 1026–1043
doi:10.1111/1751-7915.13751
Funding Information
This work was supported by the Spanish MINECO (AGL2015-71227-R to ENOLAB; BFU2016-78606-P and RYC-2014-16490 to P.C); Spanish MICIU (RTI2018-095658-B-C31 to ENOLAB); and Spanish MICINN (PID2019-110630GB-I00 to P.C). Data for this study are also supported by National Institute of General Medical Sciences (NIGMS) through a Biomedical Technology Research Resource P41 grant (P41GM111244), and by the DOE Office of Biological and Environmental Research (KP1605010).

Introduction

Laccases (benzenediol: oxygen oxidoreductases; EC 1.10.3.2) are common enzymes in nature belonging to the multicopper oxidases (MCO) group (Sirim *et al.*, 2011). They contain four copper atoms that differ in their spectroscopic and electro-paramagnetic resonance (EPR) properties: a mononuclear type 1 copper (T1Cu) that is responsible for the blue colour of these enzymes (blue laccases), with a strong electronic absorbance around 610 nm and detectable by EPR (Guan *et al.*, 2018); a type 2 copper (T2Cu), which is colourless but detectable by EPR; and two type 3 copper ions (T3Cu) showing a weak absorbance near 300 nm and are not detectable by EPR. The T1Cu accepts an electron from the substrate, while the T2Cu and the two T3Cu form a trinuclear cluster and transfer electrons from the T1Cu to an O_2 molecule, which is reduced to H_2O (Chandra and Chowdhary, 2015; Su *et al.*, 2018). Laccases possess conserved amino acid motifs responsible for binding to copper atoms that are composed mainly of His-Cys (T1Cu) and His (trinuclear T2-T3 centres) residues (Su *et al.*, 2018). Laccases catalyse direct oxidation of *ortho*- and *para*-diphenols, aminophenols, polyphenols,

Fig. 1. Multiple sequence alignment and conservation scoring of the *L. plantarum* J16, *Lactobacillus apis*-52100, *Lactococcus lactis*-9504, Pa5930 and Pp4816 laccases using Praline software (Bawono and Heringa, 2014). The sequences of *L. apis* and *L. lactis* are representative of longest and shortest C-terminus groups in LAB, surrounded respectively in red and grey in Fig. S4. The scoring scheme works from 0 for the least conserved alignment position, up to 10 for the most conserved alignment position, and the identical conserved residues are indicated by asterisks (colour scale indicated on top). Dashes indicate gaps to maximize alignment. Encased inside boxes are the motifs that form the four copper ligands and are highly conserved in laccases (conserved sequence of these motifs are HXHG, HXH, HXXHXH and HCHXXXHXXXXM/L/F (Sharma *et al*., 2007). C-terminal Met residues are highlighted in yellow, and His in purple.

polyamines and aryl diamines, as well as a few inorganic ions. Some substrates cannot be oxidized directly by laccases because of their high-redox potential or a steric hindrance. They can, however, be oxidized with the help of low-molecular-weight redox mediators (Kunamneni *et al*., 2008). Redox mediators are diffusible electron carriers, which once oxidized by laccase, can oxidize bulky or high-redox potential compounds which otherwise are not oxidized by laccase alone (Mateljak *et al*., 2019). Structurally laccases are either monomeric or homodimeric proteins with an average molecular mass of 60-100-kDa (Madhavi and Lele, 2009). They can be classified as two or three domain enzymes having the cupredoxin fold as a common signature, which suggests that this protein is the common ancestor (Chauhan *et al*., 2017). Laccase catalytic activity has been described in a wide range of biological functions such as spore resistance and pigmentation, lignification of plant cell walls, lignin biodegradation, humus turnover, detoxification processes, virulence factors and iron homoeostasis (Kunamneni *et al*., 2007). Laccases have been isolated from a range of animals, different plants, fungi and bacteria (Chauhan *et al*., 2012), although most characterized laccases were obtained from fungi, especially white-rot fungi, known as efficient lignin degraders. Bioinformatics studies on laccases have indicated that they are present in various high G + C Gram-positive bacteria and α-, γ-, and ε-proteobacteria and archaea (Alexandre and Zhulin, 2000; Sharma *et al*., 2007; Ausec *et al*., 2011). However, their possible applications are not well explored; only a few prokaryotic laccase enzymes have been purified and analysed (Sharma *et al*., 2007, Reiss *et al*., 2013, Fernandes *et al*., 2014), mainly from the genera *Bacillus* and *Streptomyces*, but also from other eubacteria and archeon species (Rosconi *et al*., 2005; Sharma *et al*., 2007; Galai *et al*., 2009; Hsiao *et al*., 2011; Reiss *et al*., 2013; Ausec *et al*., 2015; Martins *et al*., 2015; Mathews *et al*., 2016; Afreen *et al*., 2017; Basheer *et al*., 2017; Rezaei *et al*., 2017). Genes from unknown α- and γ-proteobacterium and metagenomes have been also cloned, expressed, purified and characterized (Singh *et al*., 2011a). Recently, two multicopper oxidases (MCO) from lactic acid bacteria (LAB) *Lactiplantibacillus plantarum* (basonym: *L. plantarum*) J16 and *Pediococcus acidilactici* CECT 5930 obtained from wine and cereal, respectively (Callejón *et al*., 2014), have been identified as genuine laccases (Callejón *et al*., 2016; Callejón *et al*., 2017). More recently, the characterization of a MCO from a strain of LAB *Limosilactobacillus fermentum* (basonym: *Lactobacillus fermentum*) has been reported (Xu and Fang, 2019). These three LAB enzymes have an interesting technological capacity, the degradation of biogenic amines (BA), which are toxic for humans (Ladero *et al*., 2010; Russo *et al*., 2010; Russo *et al*., 2016).

Differences between fungal and prokaryotic laccases include the cellular localization, the redox potential, optimal physicochemical reaction conditions, substrate range and the specific activity, and in some cases, tertiary structure. In biotechnological processes, mainly fungal laccases have been used (Machczynski *et al*., 2004). However, bacterial laccases could overcome some limitations of fungal laccases. In this regard, prokaryotic laccases can catalyse reactions in a wider pH range, exhibit higher thermal stability, can be more easily expressed, can feasibly be improved by genetic engineering, and are more tolerant towards organic solvents, high salt concentrations, and common laccase inhibitors than fungal enzymes (Machczynski *et al*., 2004; Gunne, 2014; Callejón *et al*., 2017). Although multiple applications have been described for bacterial laccases (Martins *et al*., 2015; Chauhan *et al*., 2017), very few have been commercialized to date.

High-resolution three-dimensional structures for bacterial laccases have been solved, with CotA from *B. subtilis* and CueO from *E. coli* being the best known (Roberts *et al*., 2002; Enguita *et al*., 2003; Hakulinen and Rouvinen, 2015). However, no three-dimensional structure of any LAB laccase has previously been determined. Here, we biochemically characterize a new laccase from *Pediococcus pentosaceus* that shows similar catalytic properties to the laccase from the previously described *P. acidilactici* (Callejón *et al*., 2017) but degrades tyramine to a higher extent. We describe the structures of both LAB laccases, which notably contain an extended Met-rich C-terminus, a feature not observed before in other laccases.

Results

Sequence analysis, cloning and expression of the *P. pentosaceus* 4816 laccase

The gene PEPE_0502 codes for a putative MCO in the *P. pentosaceus* ATCC 25745 genome (NCBI ABJ67595.1). Based on this sequence, the primers

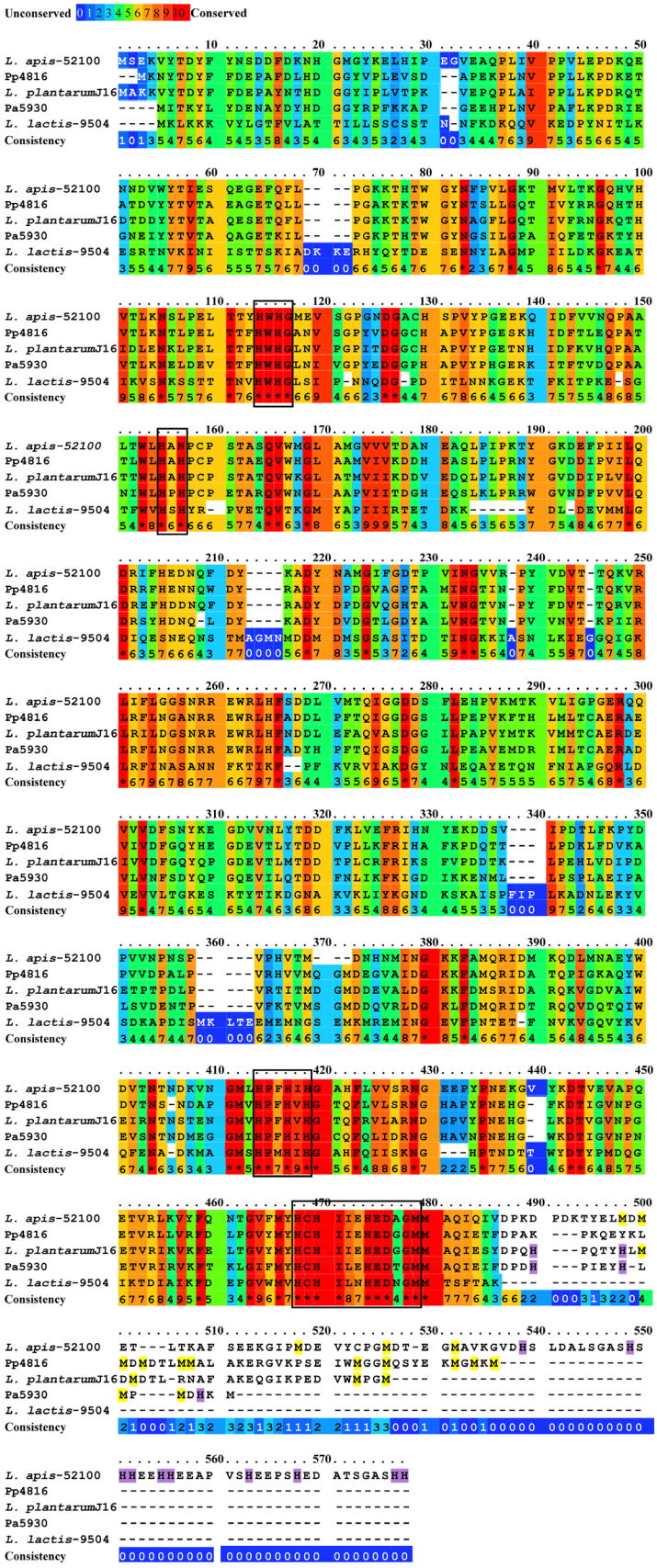

LacaPepe1 and LacaPepe2 were designed to clone the *P. pentosaceus* 4816 MCO gene, obtaining a fragment of 1800 bp. Protein sequence analysis showed the four conserved copper ligand motifs characteristic of the MCO family (Su *et al*., 2018) (Fig. 1). This protein (Pp4816) shows 59% sequence identity with the Pa5930 laccase previously described (Callejón *et al*., 2017).

The Pp4816 gene was cloned into the pET28a expression plasmid, and the resulting construct (pET28a-Pp4816) was transformed into *E. coli* BL21 (DE3) pGro7. Cell-free extracts of eleven transformed clones with or without induction by isopropyl-β-D-thiogalactopyranoside (IPTG) were analysed for ABTS oxidation activity and by SDS-PAGE. All of the induced extracts showed a strong ABTS oxidation activity and a protein band absent in non-induced extracts.

Recombinant Pp4816 laccase containing a 6xHis-tag was purified from the crude extract by metal-chelating chromatography on Ni^{2+}-NTA agarose (Fig. 2A). After purification, the amount of recombinant laccase protein from a 2 L cell culture was around 91 mg.

Characterization of the recombinant Pp4816 and Pa5930 laccases

Electrophoretic mobility on SDS-polyacrylamide gel (Fig. 2A) revealed a Pp4816 apparent molecular weight of around 64 kD, including the poly-His-tag (2.5 kD).

The purified recombinant protein showed a deep blue colour and exhibited a maximum peak at 600 nm in the UV–visible absorption spectrum (Fig. 2B), which corresponds to the characteristic T1 copper centre absorbance peak of the MCOs (Guan *et al*., 2018).

To determine kinetic parameters of recombinant Pp4816 laccase for substrate ABTS, the increase in OD_{420} over time for different substrate concentrations was recorded. Surprisingly, the experimental curve of initial rates against ABTS concentration was slightly sigmoidal. By fitting these data to an empirical equation for sigmoidal enzyme kinetics, a k_{cat} and a $K_{0.5}$ of 10.1 ± 2.5 s^{-1} and 0.31 ± 0.03 mM, respectively, were determined (Table 1). Previously, we did not appreciate a sigmoid behaviour for the homologous laccase Pa5930 (Callejón *et al*., 2017); however, after more

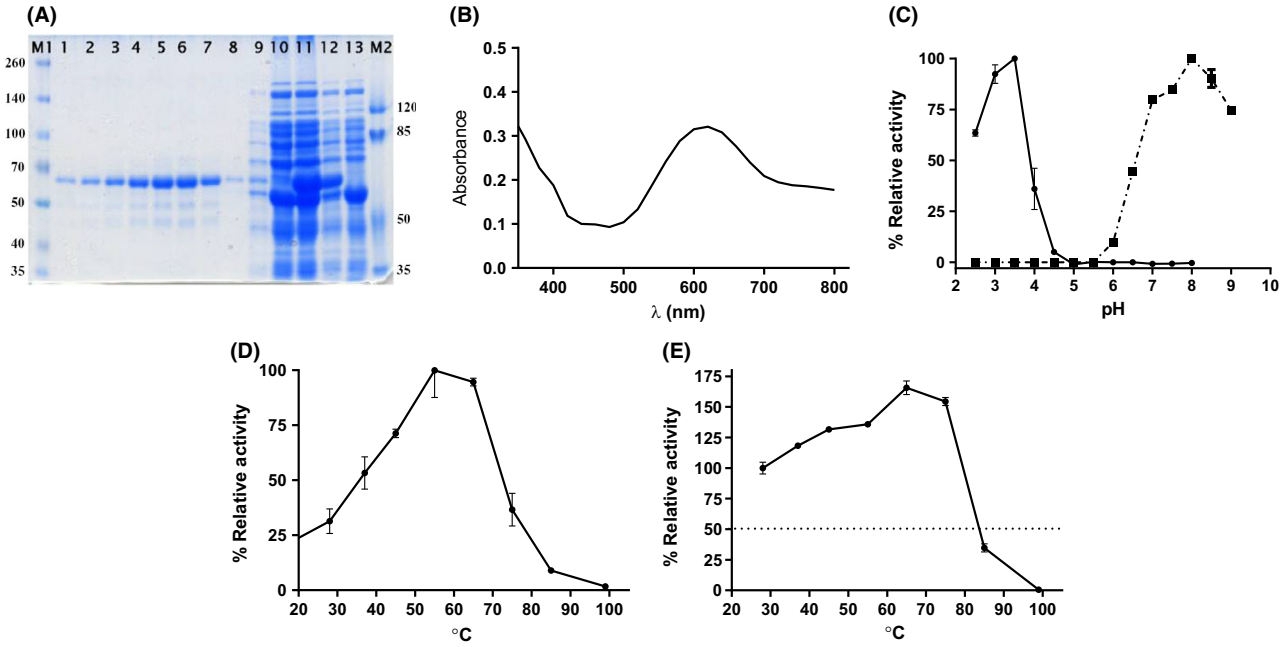

Fig. 2. Purification and biochemical characterization of Pp4816 laccase from *P. pentosaceus*.
A. Aliquots of the fractions from the different purification steps of the Pp4816 laccase were analysed by PageBlue-stained 7.5% SDS-polyacrylamide gel electrophoresis. Lane M1, Amersham™ ECL™ Rainbow™ Marker – Full range; lanes 1-8, consecutive fractions obtained after elution of the bound proteins from the Ni^{+2}-NTA agarose matrix; lane 9, column washing fraction; lane 10, unbound proteins collected in the flow-through; lane 11, crude cell extract, corresponding to the loaded sample on the column; lane 12, whole-cell proteins from an induced culture; lane 13, whole-cell proteins from a non-induced culture; and lane M2, Pierce™ Prestained Protein MW Marker.
B. UV–visible spectrum of purified recombinant Pp4816 laccase in 50 mM sodium phosphate, pH 6.5 buffer. Only the range 350-800 nm wavelength is shown.
C. pH effect on the activity of the Pp4816 enzyme towards ABTS (filled circle) and 2,6-DMP (filled square). Enzyme activity is plotted as a percentage relative to the maximum value (% relative activity). The values are means ± standard deviations from triplicate assays.
D. Temperature dependence and (E) T_{50} of the Pp4816 laccase are determined against ABTS. In D, the maximum value was assumed as 100% activity and the others were calculated proportionally. In E, relative activities were calculated considering the OD_{420} increase obtained at 28°C as 100% activity; the resulting percentages are plotted against the pretreatment temperature. The values are means ± standard deviations from triplicate assays.

Table 1. Kinetics parameters of Pp4816 and Pa5930 recombinant laccases for the substrates ABTS, 2,6-DMP and ferrocyanide.

Laccase	Substrate	K_m (mM)	k_{cat} (s^{-1})	k_{cat}/K_m (mM^{-1} s^{-1})
Pp4816	ABTS	0.31 ± 0.03[a]	10.1 ± 2.5	32.6
	2,6-DMP	6.33 ± 1.32	0.03 ± 0.004	0.005
	Ferrocyanide	0.47 ± 0.24	255.0 ± 24	542.5
Pa5930	ABTS	0.33 ± 0.04[a]	2.31 ± 0.26	7.0
	2,6-DMP	3.11 ± 0.85	0.032 ± 0.003	0.01
	Ferrocyanide	1.02 ± 0.7	87.4 ± 21	85.7

a. Both enzymes showed sigmoidal kinetic with ABTS. For this substrate, the $K_{0.5}$ (substrate concentration that generates a half-maximal velocity and is operationally similar to the Michaelis constant, K_m) was determined.

detailed kinetic analysis, sigmoidal kinetics were also found. After the sigmoidal fitting for the Pa5930 laccase, the values of k_{cat} = 2.31 ± 0.26 s^{-1} and $K_{0.5}$ = 0.33 ± 0.04 mM were obtained (Table 1). Curiously, with both enzymes, the sigmoidal kinetic profile was only observed with ABTS and not with other substrates typical of laccases as ferrocyanide and 2,6-DMP (Fig. S1). The rate data of both enzymes with these two substrates were fitted to hyperbolic curves (Fig. S1). The kinetic parameters for 2,6-DMP and ferrocyanide are shown in Table 1.

On the substrate ABTS, Pp4816 was active only at acidic pH, with a maximum around pH 3.0-3.5, and was inactive above pH 4.5. For 2,6-DMP, the maximum activity was detected around pH 8.0-8.5 (Fig. 2C), whereas no activity was detected against guaiacol in the pH range and conditions used. The optimal temperature for ABTS oxidation was in the range 55-65°C, although the enzyme showed more than 50% activity in the range of 37 to 70°C (Fig. 2D). Thermal resistance experiments showed that Pp4816 laccase is a relatively thermostable enzyme, showing a T_{50} (defined as the temperature at which the enzyme retains 50% of its activity after a 5 min incubation) of 83.7°C (Fig. 2E). Its highest activity was found after 5 min treatment at 65°C; at this temperature, the recorded activity was even higher than those found at lower temperatures. Heat treatments above 75°C dramatically decreased the laccase activity (Fig. 2E).

ABTS was a remarkably efficient mediator for 2,6-DMP oxidation at pH 4.0, and mediated oxidation of some biogenic amines (see below). We also investigated the oxidation of 2,6-DMP by both recombinant laccases using two other well-known laccase redox mediators, HBT and TEMPO, which act through distinct reaction mechanisms (Guan *et al.*, 2018). HBT and TEMPO failed, as these two compounds were not substrates of Pp4816 and Pa5916 laccases at pH 4.0 or pH 7.5 (results not shown).

Effect of putative inhibitor compounds on Pp4816 and Pa5930 laccases

Different potential inhibitors were tested on both recombinant enzymes. The enzymatic activity in the presence of 1 mM inhibitor is shown in Fig. 3. The corresponding inhibitor equivalents (inhibitor/enzyme molar ratios) were 6800 for laccase Pp4816 and 6560 for enzyme Pa5930. Semicarbazide, sodium azide and cysteine completely inhibited the ABTS-oxidizing activity of both enzymes. Bipyridil, thioglycolic acid, phenanthroline and zinc chloride diminished their activity by 50% or more, whereas clorgyline, pargyline, NaCl, NaF and EDTA decreased the activity of Pa5930 laccase but exerted a lesser inhibitory effect on Pp4816 enzyme. Cyclopropylamine, deprenyl and rasagiline decreased the activity of both laccases by less than 25%. In general, both enzymes showed similar behaviour for the tested compounds, although Pa5930 laccase seemed to be more sensitive to inhibitors, with the exception of cyclopropylamine and rasagiline.

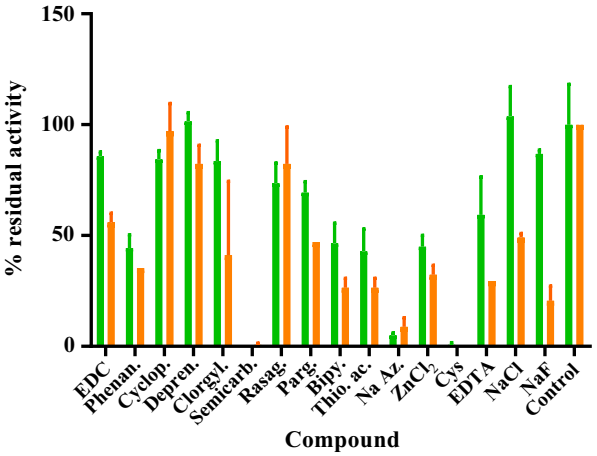

Fig. 3. Effect of different putative inhibitors on Pp4816 (green) and Pa5930 (orange) laccases. EDC: N-(3-dimethyl aminopropyl)-N'-ethyl carbodiimide; Phenan.: 1,10-phenanthroline; Cyclop.: cyclopropenyl; Depren.: deprenyl; Clorgyl.: clorgyline; Semicarb.: semicarbazide; Rasag.: rasagiline; Parg.: pargyline ; Bipy.: 2,2′-bipyridyl; Thio. ac.: thioglycolic acid; Na Az.: sodium azide; $ZnCl_2$: zinc chloride; Cys.: cysteine HCl monohydrate; EDTA: ethylenediaminetetraacetic acid; NaCl: sodium chloride; NaF: sodium fluoride; Control means an enzyme assay in absence of inhibitors. The remaining activity with the different potential inhibitors is graphed as percentage respect to the control (assumed as 100% of enzyme activity). Values are means ± standard deviations of triplicate assays.

Biogenic amine-oxidizing activity of Pa5930 and Pp4816 laccases

The activities of both laccases were tested on the biogenic amines (BA) most frequently found in foods: tyramine, histamine and putrescine. In addition, two structurally related amines have been included in the analysis: dopamine and phenylethylamine. Neither of the laccases was able to degrade histamine, putrescine, or phenylethylamine in the conditions tested, either with or without a mediator (ABTS). Both enzymes were able to oxidize tyramine, although only in the presence of mediator. After 24 h of incubation with enzyme and mediator, 93% of the tyramine was oxidized by Pp4816, while 70% was oxidized by Pa5930. Dopamine was oxidized in the presence and absence of mediator (Table 2). Pa5930 is apparently more dependent on the ABTS mediator than Pp4816. After 24 h of incubation with mediator, the degradation of dopamine was almost complete for both enzymes. However, in the absence of the ABTS mediator, the degradation of dopamine with Pa5930 laccase decreased by approximately half, while it was nearly the same with the enzyme Pp4816.

Structures of laccase Pa5930 and Pp4816

Crystals were obtained for both laccases which diffracted X-rays to 2.3 Å resolution for Pp4816 and to 2.5 Å or 2.0 Å for Pa5930 crystals grown in Tris-HCl pH 8.5 or HEPES pH 7.5 respectively (Table 3). The structure of Pa5930 (residues 1 to 477) at both pHs is similar, albeit the C-terminus which was not completely traced due to the absence of electron density, indicating that the last residues are disordered. The structure was traced till residue 461 at pH 8.5 and till residue 471 at pH 7.5 (Fig. S2). Overall, the structures of both *Pediococcus* laccases are highly similar (RMSD 0.9 Å for 456 residues) despite having an extended C-terminus for Pp4816 (Fig. 4A). Both laccases are monomeric and show three cupredoxin-like domains (Pfam CL0026), containing four copper ions bound (Fig. 4A). The overall fold and copper-binding sites are similar to laccases CueO from *E. coli* and CotA from *B. subtilis* (Enguita *et al*., 2003; Komori *et al*., 2014) (RMSD values shown at Table S1) (Fig. S3). Close examination of domain 1 (residues 1-168 for Pa5930 and residues 1-170 for Pp4816) reveals that the first N-terminal 25 residues have an extended coil conformation that lies on the protein surface, partially at the interface between domains 2 and 3 (Fig. 4B). This feature was specific for Pa5930 and Pp4816, as it is was not observed in CotA and CueO (Fig. 4B). Subsequent secondary structural elements of domain 1 are similar to CueO, with nine strands forming a β-barrel and one α-helix. Meanwhile, domain 2 (residues 174-313 for Pa5930 and 176-316 for Pp4816) contains 12 strands with a β-barrel form connected to domain 3 through a long coil region of 22 residues similarly to CueO and CotA. However, the *Pediococcus* laccases lack an extended loop connecting β20-β21 present in CueO and CotA (Fig. 4C). Domain 3 was formed by ten strands with a β-barrel form and one short α-helix followed by an extended C-terminus, a feature not present in CotA and CueO. This extension is 32-residues longer for Pp4816, which has two additional α-helices (Fig. 4C). *Pediococcus* laccases do not contain the methionine-rich region observed in domain 3 of CueO (14 Met and 5 His in 45 residues) that is proposed to bind additional coppers (Singh *et al*., 2011b), but surprisingly their C-terminus contains a high number of Met residues (Fig. 1 and S5). The C-terminus of Pp4816 contains 9 Met, though no His, vs. the rest of the protein (11 Met in 461 residues), and similarly, Pa5930 contains 3 Met and 3 His at the C-terminus vs. the rest of the protein (12 Met in 459 residues) (Figs 1, 4D and S5A). Interestingly, one α-helix at the C-terminus of Pp4816 structurally aligns with the CueO Met-rich insertion (Figs. 4C and S5A) and five Met residues formed a hydrophobic patch at the protein surface (Fig. S5B). Sequence alignment revels this Met-rich region at the C-terminus is common in LAB laccases, with some having even longer extensions than Pp4816, and some with His-rich C-termini (Fig. 1 and S4).

Copper coordination and TNC channel

The structures of laccases Pa5930/Pp4816 show one copper ion bound at the T1Cu site and three copper ions bound at the trinuclear copper centre (TNC), which

Table 2. Amine degradation by Pp4816 and Pa5930 laccases

	% Degraded amine				
Laccase	Tyramine	Histamine	Putrescine	Dopamine	Phenylethylamine
Pa5930	70[a]/0[b]	0[a,b]	0[a,b]	97[a]/55.2[b]	0[a,b]
Pp4816	93[a]/0[b]	0[a,b]	0[a,b]	100[a]/96[b]	0[a,b]

a. With ABTS as mediator.
b. Without ABTS.

Table 3. Data collection and refinement statistics for *Pediococcus* laccases

	Pa5930 pH 8.5	Pa5930 pH 7.5	Pp4816 pH 4.0	Pa5930 pH 3.0
Crystallization				
Crystallization mixture	30% PEG1000 0.1 M Tris-HCl pH 8.5	10% PEG8000 10% ethylene glycol 0.1 M HEPES pH 7.5	83 mM NaCitrate pH 4.0, 670 mM Li_2SO_4, 8 mM each: Gln, Asp, Gly, Pro	95 mM NaCitrate pH 3.0, 3.0% PEG 8000, 7.8% PEG 400, 1.2% DMSO, 114 mM Benzamidine HCL
Additions for crystal harvesting	PEG 3350 increased to 35%	PEG8000 and ethylene glycol increased to 20%	None	None
Data collection				
Wavelength (Å)	0.97925	0.97928	0.9202	0.9202
Space group	$P2_12_12_1$	$P2_12_12_1$	$P3_221$	$P2_1$
Cell dimensions				
a, *b*, *c* (Å)	51.8, 94.3, 97.6	52.1, 78.2, 162.5	127.4, 127.4, 75.3	56.,1 147.3, 65.5
α, β, γ (°)	90, 90, 90	90, 90, 90	90, 90, 120	90, 98.6, 90
Resolution (Å)	94.3-2.5 (2.5-2.6)	162.5-2.0 (2.05-2.0)	110-2.3 (2.4-2.3)	73.7-1.8(1.9-1.8)
No. reflections	12464 (14100)	304133 (21951)	29853 (2931)	96841 (9676)
R_{sym} or R_{merge}	0.14 (0.84)	0.08 (0.61)	0.34 (0.70)	0.19 (0.42)
Rpim	0.06 (0.35)	0.04 (0.29)	–	–
$I/\sigma I$	7.9 (2.2)	11.9 (2.7)	4.47 (1.76)	35.52 (0.71)
Completeness (%)	100 (100)	99.9 (99.8)	99.5 (98.3)	100 (100)
Redundancy	7.3 (7.5)	6.7 (6.3)	4.73	2.55
Refinement				
R_{work}/R_{free}	0.22/0.27	0.19/0.22	0.18/0.22	0.14/0/17
No. atoms				
Protein	3697	3792	4040	7674
Ligand/ion	4	4/4	5/2	21
Water	50	276	474	614
B-factors				
Protein	52.8	32.5	29.1	46.6
Ligand/ion	59.5	49.2/42.6	25.9	50.1
Water	41.3	38.8	28.4	53.0
R.m.s. deviations				
Bond lengths (Å)	0.003	0.004	0.002	0.032
Bond angles (°)	1.3	1.2	1.9	2.63
Ramachandran (%)				
Favoured	92.37	93.62	95.85	94.92
Allowed	7.19	5.96	3.75	4.34
Disallowed	0.44	0.43	0.40	0.74
PDB code	6Z0J	6Z0K	6XJ0	6XIZ

are distributed as one copper ion bound to the T2Cu site and a pair bound to T3Cu site (Fig. 5A). Copper coordination at the T1Cu site and the TNC is similar to CueO and CotA (Fig. S6A). The T1Cu site is located close to the protein surface at domain 3 and is coordinated by four residues His389/391, His448/450, Cys443/445, and Met453/455. In turn, the T1Cu site is connected to the TNC, which is buried at the interface of domains 1 and 3, through two adjacent His bound to the pair of coppers at the T3Cu site (Figs. 5A and S6A). As in other laccases, the TNC is surrounded by conserved negative residues Glu449/451, Asp116/118 and Asp417/419 (Fig. S6B), which have been proposed to facilitate oxygen binding and to supply protons for the reduction of oxygen. Glu seems to play a crucial role (Chen *et al.*, 2010; Komori *et al.*, 2012) as it is connected to T1Cu site through the adjacent His (Fig. S6B). Interestingly, water molecules could be modelled in the structures interacting with the TNC, one located between T3aCu and T3bCu sites and the other interacting with T2Cu (Fig. 5A). The presence of these water molecules at the TNC site was indicative of a reduced form, which could be acquired upon exposure to X-rays as evidenced in structural studies of CueO (Komori *et al.*, 2014).

Additionally, in the Pa5930 and Pp4816 structures, waters were modelled that define the channel leading to the TNC. The 32-residue C-terminal extension in Pp4816 caps this channel and appears to restrict access to it (Fig. S7). Several residues (Y502, M509 and M476), as well as the C-terminal carboxyl group, project into the entrance of the TNC channel (Fig. 5B). Pa5930 lacks this extension and has a much more exposed TNC (Fig. 5C). A search of all laccase crystal structures revealed none have significant sequence similarity to the Pp4816 C-terminus; however, the *Melanocarpus*

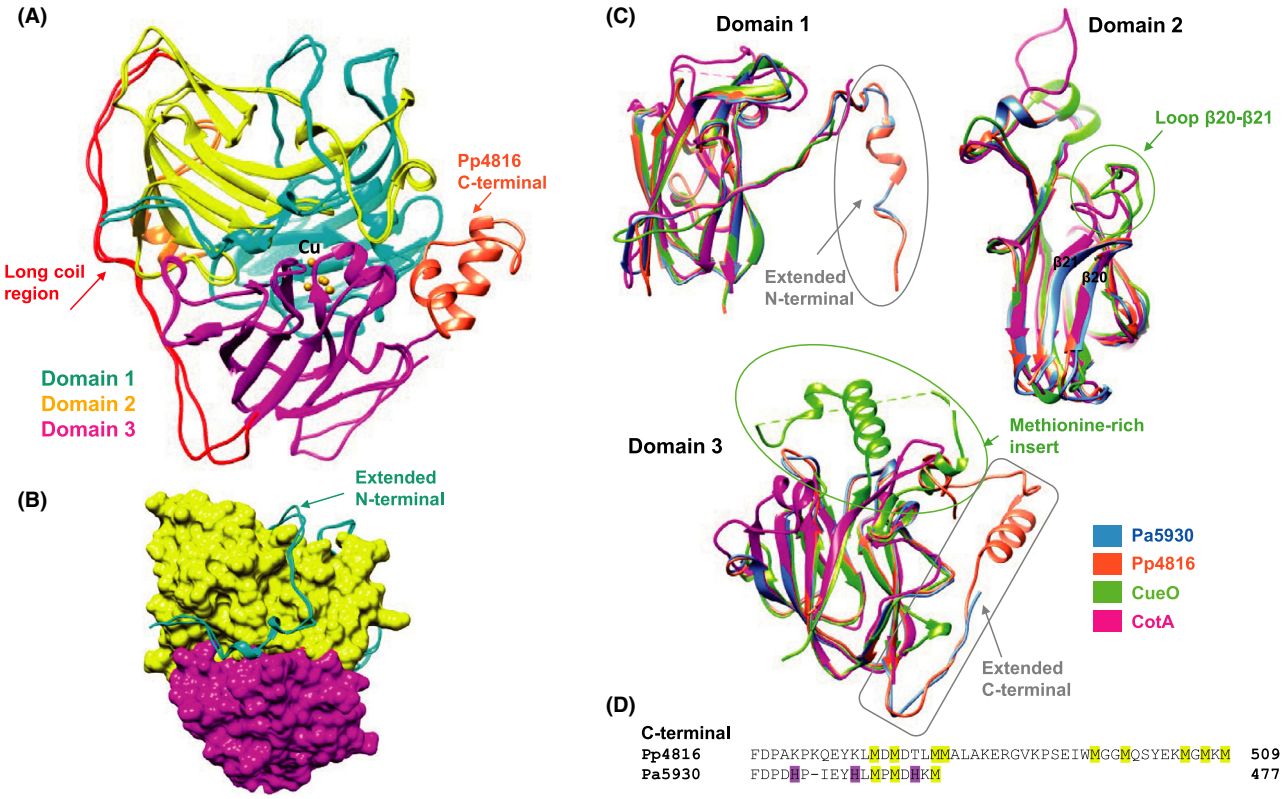

Fig. 4. Structure of *Pediococcus* laccases Pa5930 and Pp4816.
A. Structural superposition of both *Pediococcus* laccases with each cupredoxin-like domain colour-coded (1 in cyan, 2 in yellow and 3 in magenta). The long coil region connecting domain 2 with 3 is coloured in red, and the C-terminal extension of Pp416 is coloured in pale orange. The four copper ions are shown as yellow spheres.
B. Surface representation of domain 2 and cartoon representation of domain 1, all domains are colour-coded.
C. Superposition of each cupredoxin domain at *Pediococcus* laccases Pa5930 (in blue) and Pp4816 (in pale orange) together with CotA of B. subtilis (in magenta, PDB: 3ZDW) and CueO of E. coli (in green, PDB: 4E9T).
D. C-terminal sequence alignment of *Pediococcus* laccases highlighting the presence of Met (in yellow) and His (in purple) residues.

albomyces MaL laccase presents a conserved 'C-terminal plug' that occupies the TNC channel (Hakulinen *et al*., 2002). Although MaL has significant structural differences to Pp4816 before this point, both C-termini arrive at the TNC channel, with MaL's C-terminal plug more deeply penetrating the channel (Fig. 5D).

Substrate binding site

In order to trap *Pediococcus* laccases bound to substrate, co-crystallization and soaking studies were performed with Pa5930 laccase. Substrates used were ABTS, tyramine, and dopamine either alone or in complex. No substrate bound was found at the laccase structures even after direct addition to the crystals of a concentrated 100 mM stock solution or pure substrate.

Many laccases feature acidic pH optima. As Pa5930 structures were solved at basic pH (8.5 and 7.5), where Pa5930 laccase has little activity for tyramine, a second crystallization condition was found at pH 3.0, and the structure was determined to 1.8 Å (Table 3). Common laccase substrates (Table S2) were soaked into crystals or co-crystallized at 10 mM final concentration. Co-crystallization frequently resulted in low-resolution or mosaic data, but several complete data sets were obtained. No additional electron density was observed for any of these substrates. Interestingly, crystals at pH 3.0 belonged to the monoclinic space group $P2_1$ and feature two molecules in the asymmetric unit, in contrast with crystals at basic pH that belong to the orthorhombic space group $P2_12_12_1$ with one molecule in the asymmetric unit. At pH 3.0, the two molecules produced a dimeric interface stabilized by a benzamidine molecule which was essential for crystallization (Fig. S8). The dimeric interface is an artefact of crystal packing since Pa5930 was determined to be monomeric by gel filtration chromatography (data not shown) and the PISA server (Krissinel and Henrick, 2007) ruled out its stability in solution. The structures of Pa5930 at acidic and basic pH were almost identical with an RMSD of ~ 0.3 Å, aside from some slight

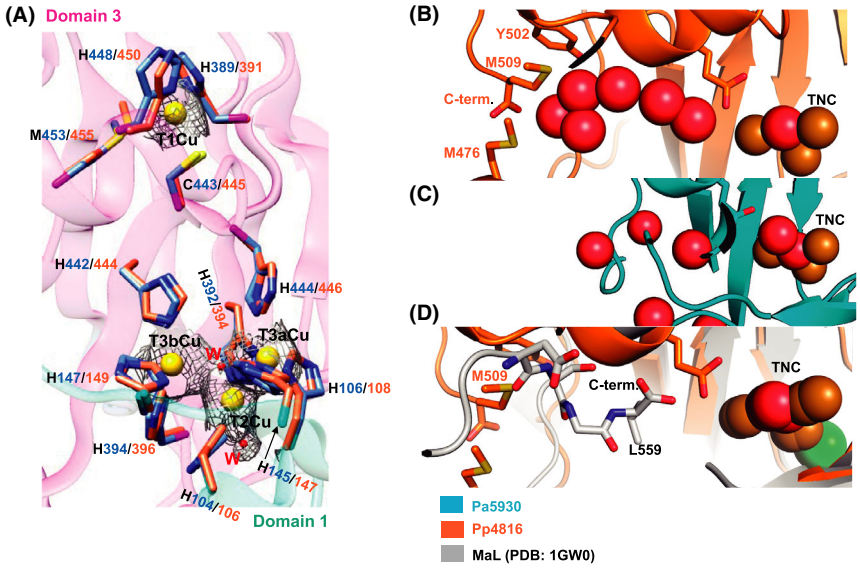

Fig. 5. Copper coordination and TNC channel. Waters observed in the crystal structures leading to the TNC are modelled as red spheres.
A. View of the T1 Cu and TNC site of coordination for superposed Pa5930 and Pp4816 laccases. Cu ions (in yellow) and water molecules at the TNC (W, in red) are rendered as spheres. The coordinating residues are colour-coded (blue for Pa5930 and pale orange for Pp4816). The cartoon represents domain 1 (in cyan) and domain 3 (in magenta), which scaffold the copper-binding motifs. The electron density map around the Cu ions is contoured at 1σ.
B. Detail of C-terminal extension of Pp4816 (orange) that caps and inserts several residues into the TNC channel (C) Pa5930 (blue) lacks this C-terminal extension and has a more exposed TNC.
D. Ascomycete laccases' C-terminal plugs (PDB 1GW0, rendered grey) penetrate the TNC channel in a similar location as Pp4816's C-terminus.

variation in loop regions involved in crystal packing. The structure at acidic pH also allowed modelling three additional residues at the C-terminus. The acidic pH-dependent activity of Pa5930 is, therefore, not mediated by major structural changes. Instead, it may be determined by protonation of key residues or the inherent increase in redox potential with decreasing pH (Brissos *et al.*, 2012).

As efforts to obtain structures of *Pediococcus* laccases bound to substrates were not successful, we superposed Pa5930 and Pp4816 with CotA structures deposited in the PDB bound to the substrates ABTS (PDB: 1OF0 and 4YVN) and sinapic acid (4Q8B) (Fig. 6A). Interestingly, CotA can bind ABTS on two different sites, one site (PDB: 3ZDW and 1OF0) is similar to sinapic acid binding (PDB: 4Q8B). This binding site is rather conserved in fungal laccases (PDB: 2HRG), and as it lies in domain 3, specifically at the entrance of T1Cu site (Enguita *et al.*, 2004) (Fig. 6B), it is proposed to be the active site where substrate oxidation can be mediated (Mehra *et al.*, 2018). The other binding site for ABTS in CotA (PDB: 4YVN) lies in the long coil region that connects domains 2 and 3 (Liu *et al.*, 2016) (Fig. 6C). The structural superposition with *Pediococcus* laccases reveals that there would be clashes for substrate binding without a change in conformation, but more importantly, the entrance of the T1Cu site is occluded by Met347/350 and Met387/389 (Fig. 6D). This feature is also observed in CueO where the methionine-rich region blocks physical access to the T1Cu site (Cortes *et al.*, 2015) (Fig. S9). In this way, substrate binding at laccases Pa5930/Pp4816 might require conformational changes for the opening of the entrance at the T1Cu site or the presence of alternative binding sites.

Discussion

The amino acid sequence of laccase Pp4816 places this enzyme into the subfamily J (bacterial CueO proteins) of the multicopper oxidases group (according to the Laccase Engineering Database) (Sirim et al., 2011), the same group that includes CueO from *E. coli* and the *L. plantarum* J16 and Pa5930 laccases. Moreover, the characteristic UV–visible spectrum with an absorption peak at 600 nm, the blue colour, and the ability to oxidize typical laccase substrates of the Pp4816 enzyme confirm it is a genuine laccase. Pp4816 and Pa5930 contain the four strictly conserved copper ligand motifs characteristics of MCO enzymes (Fig. 1) including consensus His residues, a typical trait of classical laccases (Fernandes et al., 2014; Kumar *et al.*, 2016). Pp4816 and Pa5930 have a relatively high sequence identity (59%); however, Pp4816 is closer related to the *L. plantarum* J16 laccase (66% identity) described by Callejón *et al.* (2016). It was not possible to estimate the percentage of identity of laccase Pp4816 with that of *L. fermentum* Y29 MCO recently

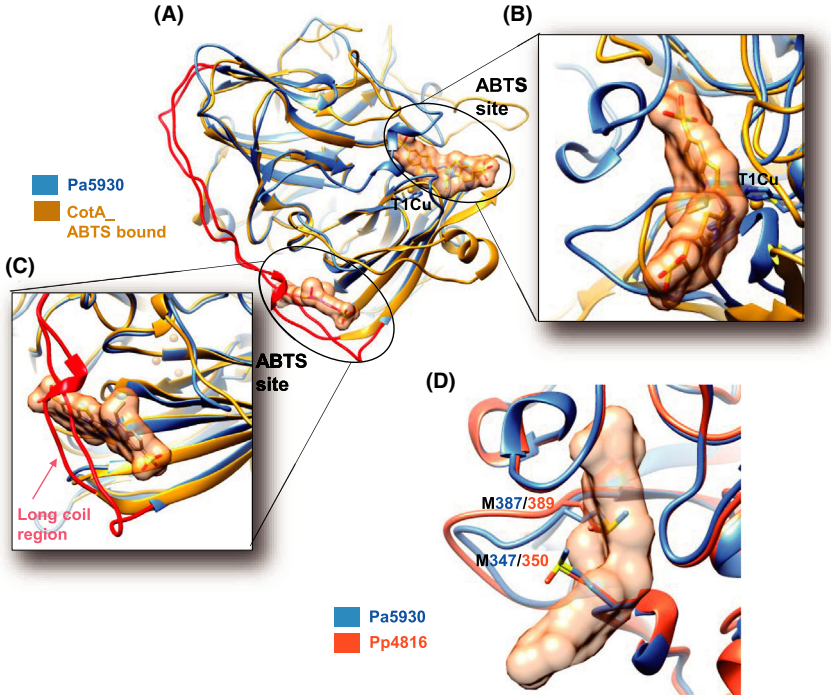

Fig. 6. Analysis of the substrate binding site in CotA with the Pa5930 and Pp4816 laccases (A) Superposition of Pa5930 (in blue) with CotA (in yellow) showing the two binding sites for ABTS (represented in atoms and transparent surface in orange). The long coil region connecting domain 2 with 3 is coloured in red in both structures.
B. Close-up of ABTS binding at the T1Cu site, the conserved laccase active site. Pa5930 shows clashes with ABTS bound to CotA.
C. Close-up of ABTS binding at an alternative site in CotA, located at the long coil region (in red) which also shows clashes with Pa5930.
D. Superposition of Pa5930 (in blue) and Pp4816 (in pale orange) laccases showing Met residues that lie at the conserved ABTS binding site close to the Cu T1 site.

published, since its gene sequence was not included in the report (nor could it be deduced from the primers described) (Xu and Fang, 2019).

The optimal pH of Pp4816 recombinant laccase acting on the non-phenolic substrate ABTS is acidic (pH 3.5), similar to that of other bacterial laccases, which ranges between 2.5 and 5.0 (Chauhan *et al*., 2017). Thermostability assays showed that Pp4816 enzyme is more resistant to high temperatures than Pa5930 and less thermostable than *L. plantarum* J16 laccase, as *L. plantarum* J16 maintains 60% activity or more up to 100°C. High thermal stabilities have been reported from various recombinant laccases: *Thermus thermophilus* SG0.5JP17-16, CotA from *B. subtilis*, *Bacillus vallismortis* fmb-103 and *Bacillus licheniformis* laccases (Martins *et al*., 2002; Lu *et al*., 2013; Liu *et al*., 2015; Sun *et al*., 2017). An amazing characteristic of Pp4816 laccase is that its activity was enhanced after pre-incubation in a temperature range between 28 and 75°C, reaching 50% more activity after 5 min at 65°C pre-incubation than after 5 min at 28°C. This behaviour could be speculatively explained because at high temperatures the protein structure undergoes conformational changes that will permit better substrate access to the active site, a Cu centres reorganizes, or inactive molecules refold. Similar behaviour was noted for the laccase of *L. plantarum* J16 (Callejón *et al*., 2016) and a number of other bacterial and fungal laccases (Mohammadian *et al*., 2010).

Strikingly, our kinetic analyses have revealed that both Pp4816 and Pa5930 laccases exhibit sigmoidal kinetics for the artificial non-phenolic substrate ABTS, which, to our knowledge, had not previously been reported for any other laccase. Generally, sigmoidicity of rate curves results in a cooperative effect in the substrate binding by multimeric enzymes (Cornish-Bowden, 2012); however, we have not found any evidence for an oligomeric structure in our crystallographic studies, nor in our size exclusion chromatography analyses, so apparently both recombinant laccases are monomeric proteins. Although rare, sigmoidal kinetics can also occur in monomeric enzymes, either reflecting substrate binding to an effector site in addition to a single active centre, or by a hysteretic mechanism, that is substrate binding to an enzyme with different conformations (Porter and Miller, 2012). We have not obtained crystals of any *Pediococcus* laccase containing ABTS bound, but since the homologous enzyme CotA is known to bind ABTS at a second site (Enguita *et al*., 2004), the first of the above

mechanisms is plausible. In any case, further studies will be required to refine the peculiar behaviour of *Pediococcus* laccases regarding the artificial substrate ABTS, and their physiological function, if any, acting on natural substrates. $K_{0.5}$ values for both Pp4816 and Pa5930 recombinant enzymes with ABTS were similar to the K_m previously determined for the *L. plantarum* J16 laccase (Callejón *et al*., 2016), although lower than the K_m of the recently described *L. fermentum* Y29 (Xu and Fang, 2019). Thus, apparently, the affinity of *Pediococcus* laccases for ABTS is higher than that of *L. plantarum* and *L. fermentum* laccases.

Low percentages of inhibition of 100 μM EDTA, EDC, bipyridyl and phenanthroline on Pa5930 laccase were recorded by Callejón *et al*. (2016). However, when 1 mM of these and other compounds was tested in the present study on both Pp4816 and Pa5930 recombinant enzymes, higher percentages of inhibition were observed. The most effective inhibitory compounds were reducing agents, such as cysteine, electron-transfer blockers to oxygen, such as azide, and also covalent modifying compounds typical of monoamine oxidases, such as semicarbazide. *Pediococcus* laccases feature inhibition similar to other diverse laccases (Singh *et al*., 2011a; Callejón *et al*., 2016; Callejón *et al*., 2017).

The new potential application, recently described, for laccase enzymes in the elimination of toxic biogenic amines (BA) in food has increased interest in LAB laccases, since LAB strains are frequently found in food. We have previously shown that the laccase of *L. plantarum* J16, a LAB strain isolated from wine, can degrade different BA (Callejón *et al*., 2016). We have found that both LAB Pp4816 and Pa5930 recombinant laccases catalyse the oxidation of dopamine and tyramine, but not histamine, phenylethylamine or putrescine. Apparently, a phenolic structure, present in dopamine and tyramine, is required to be a suitable substrate. Although the *L. plantarum* J16 laccase showed low activity on the N-heterocycle histamine, and on the aliphatic diamine putrescine, tyramine was by far the best substrate (Callejón *et al*., 2016). Together, these results indicate that just as phenolic compounds are generally better substrates for both fungal and bacterial laccases (Reiss *et al*., 2013), phenolic amines are also better for LAB laccases. Nevertheless, with both recombinant laccases, Pp4816 and Pa5930, and under the assay conditions used in this work, efficient tyramine oxidation required the presence of ABTS as a redox mediator. Dopamine was significantly oxidized in the absence of a mediator, although in the presence of ABTS its degradation was increased. The distinct suitability as a substrate for these aromatic amines could be the result of the additional -OH group adjacent to the phenoxy-OH in dopamine. In this regard, has been reported (for many different laccases) that the oxidizing activity is higher on phenolic substrates containing one or more hydroxy or methoxy group(s), with a lone pair of electrons, adjacent to the phenol (Reiss *et al*., 2011; Reiss *et al*., 2013). The laccase from *L. fermentum* Y29 has extended abilities to degrade BA; thus, it degrades histamine, tyramine, putrescine and spermidine in a similar range between 40% and 50%, and apparently in absence of any mediator compound (Xu and Fang, 2019). This high oxidizing capability on non-aromatic BA is surprising, considering that for most laccases the typical substrate is aromatic. Further work and a deeper analysis are required to understand entirely this apparently extraordinary laccase enzyme.

The structural analysis of *Pediococcus* laccases Pa5930 and Pp4816 has shown that they share similarity with other laccases such as CotA and CueO, having three cupredoxin-like domains and coordinating four Cu ions comprised at the T1Cu and TNC sites. However, the structures have revealed an extension of the C-terminus, absent in CotA and CueO, which is 32-residues longer in Pp4816 than Pa5930. Moreover, the C-terminal extension in both *Pediococcus* laccases contains a high percentage of Met and His, especially in Pp4816, where five Met form a hydrophobic patch that is surface exposed. This feature is rather common among LAB (Fig. 1), where some show a longer C-terminus rich in His. In general, all LAB laccases share a rather common general sequence, even those more distantly related (Fig. 1), indicating the C-terminus is a distinctive character among them. These C-terminal sequences are rather rich in Met and/or His, which could have a specific role *in vivo* to be determined. The presence of this Met/His rich region could be involved in additional copper-binding as a substrate docking–oxidation site for the cuprous oxidase function, as observed in CueO (Cortes *et al*., 2015), or in sequestration and transport of copper as in the copper pump CusA (Su *et al*., 2011). Indeed, in Pa5930 and Pp4816, the conserved binding site for the substrate that lies at the entrance of the T1Cu site, present in CotA and other fungal laccases (Mehra *et al*., 2018), is occupied by two Met contributing to a reduced substrate binding affinity. In fact, no substrate was found at the laccase structures despite many trials of soaking, and co-crystallization studies with different substrates were performed. However, the fact that the Met hydrophobic patch, as observed in Pp4816, is far away from the T1Cu site (~15Å) contrasts with its function as an electron-transfer mediator.

Our structural studies have also revealed that in Pp4816, the water channel leading to the TNC is capped by the C-terminal extension, similarly (but less pronounced than) the ascomycete laccase MaL. C-terminal extensions have been found to modulate the activity of several laccases; indeed, truncation of the final four residues of MaL or mutation of Leu559 (the final residue) to

Ala significantly impairs activity (Andberg *et al*., 2009). Consistent with these results, compared to Pa5930, Pp4816 shows higher thermostability, a slightly more acidic pH optimum, a bit higher activity against tyramine with mediators, and twice the activity against dopamine without mediators. Conversely, in the *Myceliophthora thermophila* laccase, which also has conserved ascomycete C-terminal plug (Ernst *et al*., 2018), mutation of a conserved Ser (which appears to form a hydrogen bond with the C-terminal plug) to Gly resulted in an increase in activity towards phenolic (8-fold) and non-phenolic (3-fold) substrates (Zumarraga *et al*., 2008). Mutation or truncation of the C-terminal residues of *Basidiomycetes* laccases also affects their activity (Pardo and Camarero, 2015), having been associated with protein processing, stability and activity, but not regulation of access to the TNC channel. The presence of the C-terminal plug in Pp4816 restricting access to the TNC could be involved in modulating its laccase activity. A similar situation could happen for other laccases possessing similar or longer C-terminal chains rich in His (Fig. 1 and S4). Thus, function and impact on the activity of the C-terminal Met/His-rich extension of these *Pediococcus* laccases as well as influence of the C-terminal plug are yet to be determined.

Experimental procedures

Chemicals and DNA and protein purification systems

2,2-azino-bis(3-ethylbenzothiazoline-6-sulfonic acid) (ABTS), 2,6-dimethoxyphenol (2,6-DMP), 1-hydroxybenzotriazole (HBT), tyramine, dopamine, phenylethylamine, putrescine, N-(3-dimethyl aminopropyl)-N′-ethylcarbodiimide (EDC), 1,10-phenanthroline, 2,2′-bipyridyl, clorgyline, cyclopropylamine, deprenyl, pargyline HCl, rasagiline, semicarbazide, NaCl, NaF and molecular weight standard proteins were obtained from Sigma-Aldrich (Madrid, Spain). 2,2,6,6-tetramethylpiperidine 1-oxyl free radical (TEMPO) was from TCI (Tokyo, Japan). Nickel-chelating nitrilotriacetic acid (Ni^{+2}-NTA) agarose was from Qiagen (Hilden, Germany). All other chemicals and reagents were of analytical grade.

Restriction enzymes were obtained from New England Biolabs (Beverly, MA, USA), T4 DNA ligase was from Roche Diagnostics (Barcelona, Spain), and DNA polymerase was from Invitrogen (La Jolla, CA, USA).

The UltraClean® PCR Clean-Up kit (Metabion) and the NZyMiniprep kit (Nzytech, Lisbon, Portugal) were used. DNA synthetic oligonucleotides were from Eurofins MWG Operon (Ebersberg, Germany).

Strains, plasmids and proteins

P. pentosaceus 4816 strain was isolated from pasta manufacturing process. *Escherichia coli* DH5α was used for cloning, amplification and propagation of the putative laccase gene. *E. coli* BL21(DE3) (Novagen, Madison, WI, USA), also harbours the pGro7 plasmid (kindly provided by R. Muñoz from ICTAN-CSIC) coding the genes of chaperones (groES–groEL) that cooperatively help the protein folding process (Thomas *et al*., 1997). The plasmid pET-28a(+) was from Novagen. Pa5930 purified laccase was previously obtained by Callejón *et al*. (2017), but a new purification was carried out for this work.

Growth conditions

P. pentosaceus 4816 was routinely cultivated in MRS medium (Scharlau S.L., Barcelona, Spain) at 28°C. *E. coli* cells were grown at 37°C in Luria–Bertani (LB) medium (Sambrook *et al*., 1989), and transformants, when appropriate, were grown in LB medium supplemented with 50 μg mL^{-1} kanamycin or with kanamycin plus 20 μg mL^{-1} of chloramphenicol.

Cloning of the gene encoding the Pp4816 laccase, construction of the expression plasmid, and expression conditions

The Pp4816 laccase gene was amplified by PCR from purified genomic DNA with newly designed primers LacaPepe1 (5'-GAT***GCTAGC***ATGAAAAACTATACG-GACTATTT-3') and LacaPepe2 (5'-CCG***GAATTC***TTA-CATTTTCATTCCCATTTT-3'). Recognition sites for NheI and EcoRI, at the start and end of the codifying sequence, are indicated in bold italics. The thermal profile set-up was as in Callejón *et al*. (2017). All the next molecular manipulations were done as described in Callejón *et al*. (2017). The recombinant laccase was cloned in pET-28a to obtain the plasmid pET-28a-Pp4816.

The expression of the two laccases was done as in Callejón *et al*. (2017), using here 0.5 mg mL^{-1} of arabinose, and 0.2 mM of $CuCl_2$.

Recombinant laccase purification

Frozen cells recovered from 2 litres culture were thawed and lysed as in Callejón *et al*. (2017) but including one cOmplete™ Protease Inhibitor Cocktail tablet (Merck). The activity of different fractions was determined in the standard reaction buffer (SRB): 100 mM sodium acetate, 0.1 mM $CuSO_4$, pH 4.0, and including 2 mM ABTS as substrate (Callejón *et al*., 2014). The rest of the steps were done as described in Callejón *et al*. (2017).

Biochemical characterization of Pp4816 laccase

The UV–visible absorption spectra (300–800 nm) of the pure recombinant Pp4816 laccase were performed as in Callejón *et al*. (2017).

The relative molecular mass of the denatured protein was determined by comparison with the migration positions of the molecular mass markers (Spectra Multicolor Marker (Thermo Scientific, Madrid, Spain) in an SDS-7.5% PAGE.

Kinetic parameters of Pp4816 and Pa5930 laccases were determined at room temperature (24°C) using different concentrations of ABTS (0.01-2 mM) or the alternative laccase substrates, potassium ferrocyanide (0.1-2 mM), and 2,6-DMP (0.4-10 mM). Assays with ABTS and ferrocyanide were carried out in 50 mM sodium citrate buffer, pH 3.4, and reactions were followed by registering OD_{420} on a Beckman Coulter DU800 UV/Vis spectrophotometer. With 2,6-DMP, 50 mM Tris·HCl buffer, pH 7.2 was used, and its oxidation was determined by the OD_{468} increase. Previously, the linear dependence of the enzymatic activity with recombinant enzyme concentration was checked. Reactions were performed in a total volume of 600 μL and were initiated by the addition of the enzymes. The steady-state reaction rates were obtained from the initial slope of the linear section after plotting OD vs. time. All determinations were carried out at least in triplicates and also with different final concentrations of the recombinant laccases, in particular, between 0.05 and 0.2 μg mL^{-1} with ABTS; between 1.66 and 3.33 μg mL^{-1} with ferrocyanide; and 20-80 μg mL^{-1} with 2,6-DPM. Enzyme activity is expressed in units (U), defined as the amount of active enzyme that oxidizes 1 μmol of substrate min^{-1}. The extinction coefficients used, corresponding to the oxidation products, were as follows: ABTS, $\varepsilon_{420} = 36000\ M^{-1}\ cm^{-1}$; $K_4[Fe(CN_6)]$, $\varepsilon_{420} = 880\ M^{-1}\ cm^{-1}$; and 2,6-DMP, $\varepsilon_{468} = 14\ 800\ M^{-1}\ cm^{-1}$.

Activity of Pp4816 and Pa5930 laccases on HBT and TEMPO, as potential substrates, was tested as described by Ander and Messner (1998) and Kulys and Vidziunaite (2005), respectively. The assays were carried out, with the recombinant laccases at a final concentration of 30 μg mL^{-1}, in two different buffers: 50 mM sodium citrate, pH 4.0, and 50 mM Tris·H_2SO_4, pH 7.5. In these assays, commercial *Trametes versicolor* laccase (Sigma), at 3 μg mL^{-1}, was used as a positive activity control. ABTS, HBT and TEMPO were also tested as mediators of both laccases for the oxidation of 2,6-DMP at pH 4.0. For these trials, the reaction mixtures contained 50 μg mL^{-1} of enzyme, 4 mM 2,6-DMP and 0.5 mM of the potential mediators in sodium citrate buffer, pH 4.0. 2,6-DMP oxidation was followed by DO_{468}. Samples in which any mediator was omitted were negative controls.

To determine the effect of pH on laccase activity with ABTS (2 mM), 2,6-DMP (4 mM) and guaiacol (40 mM) as substrates, a 50 mM citrate–phosphate buffer, 0.1 mM $CuSO_4$, was used, covering a pH range from 2.5 to 9.0. Final laccase concentration was 5.5 μg mL^{-1} with ABTS; and 36.6 μg mL^{-1} with 2,6-DMP and guaiacol. Enzyme activity on these substrates was determined spectrophotometrically at an OD_{420} for ABTS and guaiacol and OD_{468} for 2,6-DMP during 30 min incubation at room temperature. The effect of temperature on Pp4816 laccase activity in the range 20–100°C was checked by measuring ABTS oxidation using 200 μL of SRB plus 2 mM ABTS to which 1 μL of an enzyme solution of (365 μg mL^{-1}) was added. The reaction medium was pre-incubated for 5 min at the corresponding temperatures before the addition of the recombinant enzyme. For thermal stability analysis, 200 μL of SRB plus 10 μL of an enzyme solution (91 μg mL^{-1}) was pre-incubated at the different temperatures ranging from 28 to 85°C for 5 min. After recovering the room temperature, reactions were initiated by the inclusion of ABTS at the final concentration of 2 mM.

In temperature and thermal stability analyses, reactions were developed for 3 min then stopped by adding sodium azide to a final concentration of 1 mM. Oxidation of ABTS was measured by recording the increase of OD_{420} in microplate wells.

Effect of putative inhibitor compounds on Pp4816 and Pa5930 laccases

The effect of metal-chelating agents 2,2′-bipyridyl, and EDTA; compounds affecting the oxidizing potential of the enzyme clorgyline, cyclopropylamine, deprenyl, EDC, pargyline, phenanthroline, rasagiline, semicarbazide, and sodium azide; halides such as sodium fluoride and chloride, which bind to the T2 copper prohibiting oxygen from being reduced; and reducing agents cysteine and thioglycolic acid, and also Zn^{2+}, with potential for substitution of Cu^{2+}, provided as zinc chloride, was tested on the recombinant laccase Pp4816 similarly as was previously examined on Pa5930 laccase (Callejón *et al.*, 2017). After incubating 10 μL of a 183 μg mL^{-1} enzyme solution with 190 μL SRB plus 1 mM inhibitor for 10 min, reaction was initiated by the addition of ABTS (2 mM final concentration) and let to progress for 3 min when was stopped by adding sodium azide to a final concentration of 1 mM. Oxidation of ABTS was measured by recording the increase of OD_{420} in microplate wells. The value from a reaction without inhibitor was considered as 100 % relative enzyme activity (control).

Activity of Pp4816 and Pa5930 laccases on biogenic amines

Histamine, tyramine, putrescine, dopamine and phenylethylamine, in the presence and absence of the mediator ABTS, were tested as potential substrates. Incubations were carried out with 100 μL of SRB containing the amine at a final concentration of 150 μg mL^{-1}, and in the presence/absence of 2 mM ABTS. Pa5930

and Pp4816 concentrations in the reaction mix were 33.76 and 29.9 μg mL^{-1} respectively. Reaction mixtures were incubated at 28°C for 24 h, after which the remaining amine concentration was determined by LC-FLD (Callejón *et al*., 2016). As negative controls, mixtures without enzyme or with a heat-inactivated enzyme (100°C for 10 min) were tested under identical conditions.

Crystallization, data collection, model building and analysis

For crystallization of laccase Pa5930, first, gel filtration was performed in 50 mM Tris-HCl pH 7.5 and 250 mM NaCl using a ProteoSEC 6-600 kDa HR column (Generon). Different fractions were collected and run in a 12% SDS-PAGE gel, then were concentrated with Vivaspin 20 concentrators (Sartorius). Crystals of Pa5930 were prepared at the IBV-CSIC Crystallogenesis Facility by the sitting-drop vapour-diffusion crystallization technique at 21°C, mixing 0.3 μL of protein solution at 10 mg mL^{-1} with 0.3 μL of different reservoir solutions. The best diffracting crystals were grown and cryoprotected in the conditions shown in Table 3. Crystals of Pp4680 and Pa5930 at pH 3.0 were prepared at the NSLS-II acoustic sample preparation facility. An Echo™ (Labcyte) was used to assemble hanging-drop vapour-diffusion crystal trials on 3D printed tray (Soares *et al*., 2018) from aliquots of solutions in a source plate. Pp4816 formed crystals overnight at 20°C in a 60 nL drop. The largest single crystals were obtained with protein serially diluted from 20 mg mL^{-1} in water (final conditions in Table 3). Mylar was used as the tray surface, and 2 M lithium sulfate was the reservoir solution. Pa5930 (pH 3.0) also crystalized in a combinatorial screen at 5-15 mg mL^{-1}, with a tray reservoir solution of 15% PEG8000 and 15% PEG400. Mylar was initially used as the surface, resulting in micro-polycrystalline needles. Changing the surface to COC (cyclic olefin copolymer) resulted in large high-quality single crystals.

Diffraction of Pa5930 crystals at basic pH was performed under cryogenic conditions at beamline I24 at Diamond Light Source Synchrotron (DLS, Didcot, UK) and BL13-XALOC at Spanish Synchrotron Radiation Facility ALBA (ALBA, Cerdanyola del Vallès, Spain) while diffraction of Pp4816 and Pa5930 at pH 3 crystals was performed under cryogenic conditions at 17-ID-1 (AMX) at NSLS-II. Crystallographic data collected at the Diamond light source were processed with the XDS Program Package (Kabsch, 2010) and scaled with the program AIMLESS from the Collaborative Computational Project, Number 4, CCP4 suite (Winn *et al*., 2011). Data collected at the NSLS-II were indexed and scaled with *FastDP* (Winter and McAuley, 2011). For phasing, molecular replacement was conducted using Phaser (McCoy *et al*., 2007) and CotA (PDB: 3ZDW) as the search model. The final structure was obtained upon iterative cycles of tracing and refinement using COOT (Emsley *et al*., 2010) and Refmac5 (Murshudov *et al*., 2011) respectively. Details of the data collection and refinement are shown in Table 3. To note, Pa5930 crystals soaked with substrate proved to be more resistant during incubation in crystals grown at pH 7.5. Superpositions were produced with program Superpose in the CCP4 Suite. Figures were produced using UCSF Chimera (Pettersen *et al*., 2004).

Acknowledgements

This work was supported by the Spanish MINECO (AGL2015-71227-R to ENOLAB; BFU2016-78606-P and RYC-2014-16490 to P.C); Spanish MICIU (RTI2018-095658-B-C31 to ENOLAB); and Spanish MICINN (PID2019-110630GB-I00 to P.C). We would like to thank The IBV-CSIC Crystallogenesis Facility for protein crystallization screenings and local contact and staffs of the beamline BL13-XALOC and I24 at ALBA and DLS synchrotrons, respectively, for providing assistance during data collection. X-ray diffraction data collection was supported by Diamond Light Source block allocation group (BAG) Proposal MX14739 and MX20229 and Spanish Synchrotron Radiation Facility ALBA Proposal 2017072262 and 2018072901. We would like to thank two Department of Energy Visiting Faculty Program supported interns, Elizabeth Coler and Shahla Partowmah, for assisting with the crystallization and data collection of Pp4816 and Pa5930 at pH 3.0. This work was supported by a Visiting Faculty Program – DOE to R.E.C., S.P. and E.A.C; and a Quinnipiac University Faculty Grant-in-aid to R.E.C. The Visiting Faculty Program is supported through the U.S. Department of Energy, Office of Science, Office of Workforce Development for Teachers and Scientists (WDTS). Data for this study were collected at 17-ID-1 (AMX) of the National Synchrotron Light Source II, a U.S. Department of Energy (DOE) Office of Science User Facility operated for the DOE Office of Science by Brookhaven National Laboratory under Contract No. DE-SC0012704. Data for this study are also supported by National Institute of General Medical Sciences (NIGMS) through a Biomedical Technology Research Resource P41 grant (P41GM111244), and by the DOE Office of Biological and Environmental Research (KP1605010).

Conflict of interest

None declared.

Data Availability Statement

The X-ray crystallographic coordinates for the laccase structures have been deposited at the Protein Data Bank with the following accession codes: Pa5930 at pH 8.5 as 6Z0J, at pH 7.5 as 6Z0K and pH 3.0 as 6XJ0 and Pp4816 as 6XIZ.

References

Afreen, S., Shamsi, T.N., Baig, M.A., Ahmad, N., Fatima, S., Qureshi, M.I., *et al*. (2017) A novel multicopper oxidase (laccase) from cyanobacteria: Purification, characterization with potential in the decolorization of anthraquinonic dye. *PLoS One* **12:** e0175144.

Alexandre, G., and Zhulin, I.B. (2000) Laccases are widespread in bacteria. *Trends Biotechnol* **18:** 41–42.

Andberg, M., Hakulinen, N., Auer, S., Saloheimo, M., Koivula, A., Rouvinen, J., and Kruus, K. (2009) Essential role of the C-terminus in *Melanocarpus albomyces* laccase for enzyme production, catalytic properties and structure. *FEBS J* **276:** 6285–6300.

Ander, P., and Messner, K. (1998) Oxidation of 1-hydroxybenzotriazole by laccase and lignin peroxidase. *Biotechnol Tech* **12:** 191–195.

Ausec, L., Črnigoj, M., Šnajder, M., Ulrih, N., and Mandic-Mulec, I. (2015) Characterization of a novel high-pH-tolerant laccase-like multicopper oxidase and its sequence diversity in *Thioalkalivibrio* sp. *Appl Microbiol Biotechnol* **99:** 9987–9999.

Ausec, L., Zakrzewski, M., Goesmann, A., Schlüter, A., and Mandic-Mulec, I. (2011) Bioinformatic analysis reveals high diversity of bacterial genes for laccase-like enzymes. *PLoS One* **6:** 1–9.

Basheer, S., Rashid, N., Ashraf, R., Akram, M.S., Siddiqui, M.A., Imanaka, T., and Akhtar, M. (2017) Identification of a novel copper-activated and halide-tolerant laccase in *Geobacillus thermopakistaniensis*. *Extremophiles* **21:** 563–571.

Bawono, P., and Heringa, J. (2014) PRALINE: a versatile multiple sequence alignment toolkit. In: *Multiple Sequence Alignment Methods*. New York, NY: Springer, pp. 245-262.

Brissos, V., Chen, Z., and Martins, L.O. (2012) The kinetic role of carboxylate residues in the proximity of the trinuclear centre in the O_2 reactivity of CotA-laccase. *Dalton T* **41:** 6247–6255.

Callejón, S., Sendra, R., Ferrer, S., and Pardo, I. (2014) Identification of a novel enzymatic activity from lactic acid bacteria able to degrade biogenic amines in wine. *Appl Microbiol Biotechnol* **98:** 185–198.

Callejón, S., Sendra, R., Ferrer, S., and Pardo, I. (2016) Cloning and characterization of a new laccase from *Lactobacillus plantarum* J16 CECT 8944 catalyzing biogenic amines degradation. *Appl Microbiol Biotechnol* **100:** 3113–3124.

Callejón, S., Sendra, R., Ferrer, S., and Pardo, I. (2017) Recombinant laccase from *Pediococcus acidilactici* CECT 5930 with ability to degrade tyramine. *PLoS One* **12:** e0186019.

Chandra, R., and Chowdhary, P. (2015) Properties of bacterial laccases and their application in bioremediation of industrial wastes. *Environ Sci-Process Impacts* **17:** 326–342.

Chauhan, P.S., Goradia, B., and Saxena, A. (2017) Bacterial laccase: recent update on production, properties and industrial applications. *3 Biotech* **7:** 323.

Chauhan, P., Puri, N., Sharma, P., and Gupta, N. (2012) Mannanases: microbial sources, production, properties and potential biotechnological applications. *Appl Microbiol Biotechnol* **93:** 1817–1830.

Chen, Z., Durão, P., Silva, C.S., Pereira, M.M., Todorovic, S., Hildebrandt, P., *et al*. (2010) The role of Glu498 in the dioxygen reactivity of CotA-laccase from *Bacillus subtilis*. *Dalton T* **39:** 2875–2882.

Cornish-Bowden, A. (2012) *Fundamentals of Enzyme Kinetics*, 4th edn. Weinheim: Wiley-VCH Verlag GmbH & Co. KGaA.

Cortes, L., Wedd, A.G., and Xiao, Z. (2015) The functional roles of the three copper sites associated with the methionine-rich insert in the multicopper oxidase CueO from *E. coli*. *Metallomics* **7:** 776–785.

Emsley, P., Lohkamp, B., Scott, W.G., and Cowtan, K. (2010) Features and development of Coot. *Acta Crystallogr Sect D Biol Crystallogr* **66:** 486–501.

Enguita, F.J., Marçal, D., Martins, L.O., Grenha, R., Henriques, A.O., Lindley, P.F., and Carrondo, M.A. (2004) Substrate and dioxygen binding to the endospore coat laccase from *Bacillus subtilis*. *J Biol Chem* **279:** 23472–23476.

Enguita, F.J., Martins, L.O., Henriques, A.O., and Carrondo, M.A. (2003) Crystal structure of a bacterial endospore coat component: a laccase with enhanced thermostability properties. *J Biol Chem* **278:** 19416–19425.

Ernst, H.A., Jørgensen, L.J., Bukh, C., Piontek, K., Plattner, D.A., Østergaard, L.H., *et al*. (2018) A comparative structural analysis of the surface properties of asco-laccases. *PLoS One* **13:** e0206589.

Fernandes, T.A.R., Silveira, W.B.D., Passos, F.M.L., and Zucchi, T.D. (2014) Laccases from *Actinobacteria*—What we have and what to expect. *Adv Microbiol* **4:** 285–296.

Galai, S., Limam, F., and Marzouki, M.N. (2009) A new *Stenotrophomonas maltophilia* strain producing laccase. Use in decolorization of synthetics dyes. *Appl Biochem Biotechnol* **158:** 416–431.

Guan, Z.-B., Luo, Q., Wang, H.-R., Chen, Y., and Liao, X.-R. (2018) Bacterial laccases: promising biological green tools for industrial applications. *Cell Mol Life Sci* **75:** 3569–3592.

Gunne, M. (2014) *Identification and optimization of novel bacterial laccases*. Ph.D. Thesis. Heinrich-Heine-Universität Düsseldorf.

Hakulinen, N., Kiiskinen, L.L., Kruus, K., Saloheimo, M., Paananen, A., Koivula, A., and Rouvinen, J. (2002) Crystal structure of a laccase from *Melanocarpus albomyces* with an intact trinuclear copper site. *Nat Struct Biol* **9:** 601–605.

Hakulinen, N., and Rouvinen, J. (2015) Three-dimensional structures of laccases. *Cell Mol Life Sci* **72:** 857–868.

Hsiao, Y.-M., Liu, Y.-F., Lee, P.-Y., Hsu, P.-C., Tseng, S.-Y., and Pan, Y.-C. (2011) Functional characterization of copA gene encoding multicopper oxidase in *Xanthomonas campestris* pv. *campestris*. *J Agric Food Chem* **59:** 9290–9302.

Kabsch, W. (2010) XDS. *Acta Crystallogr Sect D Struct Biol* **66:** 125–132.

Komori, H., Sugiyama, R., Kataoka, K., Higuchi, Y., and Sakurai, T. (2012) An O-centered structure of the trinuclear copper center in the Cys500Ser/Glu506Gln mutant of CueO and structural changes in low to high X-ray dose conditions. *Angew Chem Int Ed* **51:** 1861–1864.

Komori, H., Sugiyama, R., Kataoka, K., Miyazaki, K., Higuchi, Y., and Sakurai, T. (2014) New insights into the catalytic active-site structure of multicopper oxidases. *Acta Crystallogr Sect D Struct Biol* **70:** 772–779.

Krissinel, E., and Henrick, K. (2007) Inference of macromolecular assemblies from crystalline state. *J Mol Biol* **372:** 774–797.

Kulys, J., and Vidziunaite, R. (2005) Kinetics of laccase-catalysed TEMPO oxidation. *J Mol Catal B: Enzym* **37:** 79–83.

Kumar, S., Jain, K.K., Rani, S., Bhardwaj, K.N., Goel, M., and Kuhad, R.C. (2016) *In-Vitro* refolding and characterization of recombinant laccase (CotA) from *Bacillus pumilus* MK001 and its potential for phenolics degradation. *Mol Biotechnol* **58:** 789–800.

Kunamneni, A., Ballesteros, A., Plou, F. J., and Alcalde, M. (2007) Fungal laccase - a versatile enzyme for biotechnological applications. In: Vilas, A.M. (ed). *Communicating Current Research and Educational Topics and Trends in Applied Microbiology*. Badajoz: Formatex, pp. 233–245.

Kunamneni, A., Camarero, S., Garcia-Burgos, C., Plou, F., Ballesteros, A., and Alcalde, M. (2008) Engineering and applications of fungal laccases for organic synthesis. *Microb Cell Fact* **7:** 32.

Ladero, V., Calles-Enriquez, M., Fernandez, M., and Alvarez, M. (2010) Toxicological effects of dietary biogenic amines. *Curr Nutr Food Sci* **6:** 145–156.

Liu, H., Cheng, Y., Du, B., Tong, C., Liang, S., Han, S., *et al*. (2015) Overexpression of a novel thermostable and chloride-tolerant laccase from *Thermus thermophilus* SG0.5JP17-16 in *Pichia pastoris* and its application in synthetic dye decolorization. *PLoS One* **10:** e0119833.

Liu, Z., Xie, T., Zhong, Q., and Wang, G. (2016) Crystal structure of CotA laccase complexed with 2,2-azinobis-(3-ethylbenzothiazoline-6-sulfonate) at a novel binding site. *Acta Crystallogr F Struct Biol Commun* **72:** 328–335.

Lu, L., Wang, T.-N., Xu, T.-F., Wang, J.-Y., Wang, C.-L., and Zhao, M. (2013) Cloning and expression of thermo-alkali-stable laccase of *Bacillus licheniformis* in *Pichia pastoris* and its characterization. *Bioresour Technol* **134:** 81–86.

Machczynski, M.C., Vijgenboom, E., Samyn, B., and Canters, G.W. (2004) Characterization of SLAC: A small laccase from *Streptomyces coelicolor* with unprecedented activity. *Protein Sci* **13:** 2388–2397.

Madhavi, V., and Lele, S.S. (2009) Laccase: properties and applications. *BioResources* **4:** 1694–1717.

Martins, L.O., Durão, P., Brissos, V., and Lindley, P.F. (2015) Laccases of prokaryotic origin: enzymes at the interface of protein science and protein technology. *Cell Mol Life Sci* **72:** 911–922.

Martins, L.O., Soares, C.M., Pereira, M.M., Teixeira, M., Costa, T., Jones, G.H., and Henriques, A.O. (2002) Molecular and biochemical characterization of a highly stable bacterial laccase that occurs as a structural component of the *Bacillus subtilis* endospore coat. *J Biol Chem* **277:** 18849–18859.

Mateljak, I., Monza, E., Lucas, M.F., Guallar, V., Aleksejeva, O., Ludwig, R., *et al*. (2019) Increasing redox potential, redox mediator activity, and stability in a fungal laccase by computer-guided mutagenesis and directed evolution. *ACS Catalysis* **9:** 4561–4572.

Mathews, S.L., Smithson, C.E., and Grunden, A.M. (2016) Purification and characterization of a recombinant laccase-like multi-copper oxidase from *Paenibacillus glucanolyticus* SLM1. *J Appl Microbiol* **121:** 1335–1345.

McCoy, A.J., Grosse-Kunstleve, R.W., Adams, P.D., Winn, M.D., Storoni, L.C., and Read, R.J. (2007) Phaser crystallographic software. *J Appl Crystallogr* **40:** 658–674.

Mehra, R., Muschiol, J., Meyer, A.S., and Kepp, K.P. (2018) A structural-chemical explanation of fungal laccase activity. *Sci Rep* **8:** 17285.

Mohammadian, M., Fathi-Roudsari, M., Mollania, N., Badoei-Dalfard, A., and Khajeh, K. (2010) Enhanced expression of a recombinant bacterial laccase at low temperature and microaerobic conditions: purification and biochemical characterization. *J Ind Microbiol Biotechnol* **37:** 863–869.

Murshudov, G.N., Skubák, P., Lebedev, A.A., Pannu, N.S., Steiner, R.A., Nicholls, R.A., *et al*. (2011) REFMAC5 for the refinement of macromolecular crystal structures. *Acta Crystallogr Sect D Biol Crystallogr* **67:** 355–367.

Pardo, I., and Camarero, S. (2015) Laccase engineering by rational and evolutionary design. *Cell Mol Life Sci* **72:** 897–910.

Pettersen, E.F., Goddard, T.D., Huang, C.C., Couch, G.S., Greenblatt, D.M., Meng, E.C., and Ferrin, T.E. (2004) UCSF Chimera-A visualization system for exploratory research and analysis. *J Comput Chem* **25:** 1605–1612.

Porter, C.M., and Miller, B.G. (2012) Cooperativity in monomeric enzymes with single ligand-binding sites. *Bioorg Chem* **43:** 44–50.

Reiss, R., Ihssen, J., and Thony-Meyer, L. (2011) *Bacillus pumilus* laccase: a heat stable enzyme with a wide substrate spectrum. *BMC Biotechnol* **11:** 9.

Reiss, R., Ihssen, J., Richter, M., Eichhorn, E., Schilling, B., and Thöny-Meyer, L. (2013) Laccase *versus* laccase-like multi-copper oxidase: a comparative study of similar enzymes with diverse substrate spectra. *PLoS One* **8:** e65633.

Rezaei, S., Shahverdi, A.R., and Faramarzi, M.A. (2017) Isolation, one-step affinity purification, and characterization of a polyextremotolerant laccase from the halophilic bacterium *Aquisalibacillus elongatus* and its application in the delignification of sugar beet pulp. *Bioresour Technol* **230:** 67–75.

Roberts, S.A., Weichsel, A., Grass, G., Thakali, K., Hazzard, J.T., Tollin, G., *et al*. (2002) Crystal structure and electron transfer kinetics of CueO, a multicopper oxidase required for copper homeostasis in *Escherichia coli*. *Proc Natl Acad Sci USA* **99:** 2766–2771.

Rosconi, F., Fraguas, L.F., Martínez-Drets, G., and Castro-Sowinski, S. (2005) Purification and characterization of a periplasmic laccase produced by *Sinorhizobium meliloti*. *Enzyme Microb Technol* **36:** 800–807.

Russo, P., Capozzi, V., Spano, G., Corbo, M.R., Sinigaglia, M., and Bevilacqua, A. (2016) Metabolites of microbial origin with an impact on health: ochratoxin A and biogenic amines. *Front Microbiol* **7:** 482.

Russo, P., Spano, G., Arena, M., Capozzi, V., Grieco, F., and Beneduce, L. (2010) Are consumers aware of the risks related to biogenic amines in food?.? In: *Current Research, Technology and Education Topics in Applied Microbiology and Microbial Biotechnology*. Méndez-Vilas, A. (ed). Badajoz: Formatex, pp. 1087–1095.

Sambrook, J., Fristch, E.F., and Maniatis, T. (1989) *Molecular cloning: a laboratory manual*, 2nd edn. Cold Spring Harbor, New York: Cold Spring Harbor Laboratory Press.

Sharma, P., Goel, R., and Capalash, N. (2007) Bacterial laccases. *World J Microbiol Biotechnol* **23:** 823–832.

Singh, G., Bhalla, A., Kaur, P., Capalash, N., and Sharma, P. (2011a) Laccase from prokaryotes: a new source for an old enzyme. *Rev Environ Sci Bio/Technol* **10:** 309–326.

Singh, S.K., Roberts, S.A., McDevitt, S.F., Weichsel, A., Wildner, G.F., Grass, G.B., *et al*. (2011b) Crystal structures of multicopper oxidase CueO bound to copper(I) and silver(I): functional role of a methionine-rich sequence. *J Biol Chem* **286:** 37849–37857.

Sirim, D., Wagner, F., Wang, L., Schmid, R. D., and Pleiss, J. (2011) *The Laccase Engineering Database: a classification and analysis system for laccases and related multicopper oxidases*. Database 2011: bar006.

Soares, A., Joshi, K., Teplitsky, E., and Zipper, L. E. (2018) *Flex Plate with Removable Inserts and Cover. United States*. Upton, NY: Brookhaven Science Associates, LLC.

Su, C.-C., Long, F., and Yu, E.W. (2011) The Cus efflux system removes toxic ions via a methionine shuttle. *Protein Sci* **20:** 6–18.

Su, J., Fu, J., Wang, Q., Silva, C., and Cavaco-Paulo, A. (2018) Laccase: a green catalyst for the biosynthesis of poly-phenols. *Crit Rev Biotechnol* **38:** 294–307.

Sun, J., Zheng, M., Lu, Z., Lu, F., and Zhang, C. (2017) Heterologous production of a temperature and pH-stable laccase from *Bacillus vallismortis* fmb-103 in *Escherichia coli* and its application. *Process Biochem* **55:** 77–84.

Thomas, J.G., Ayling, A., and Baneyx, F. (1997) Molecular chaperones, folding catalysts, and the recovery of active recombinant proteins from *E. coli*. *Appl Biochem Biotechnol* **66:** 197–238.

Winn, M.D., Ballard, C.C., Cowtan, K.D., Dodson, E.J., Emsley, P., Evans, P.R., *et al*. (2011) Overview of the CCP4 suite and current developments. *Acta Crystallogr Sect D Biol Crystallogr* **67:** 235–242.

Winter, G., and McAuley, K.E. (2011) Automated data collection for macromolecular crystallography. *Methods* **55:** 81–93.

Xu, J., and Fang, F. (2019) Expression and characterization of a multicopper oxidase from *Lactobacillus fermentum*. *Sheng Wu Gong Cheng Xue Bao* **35:** 1286–1294.

Zumarraga, M., Vaz Dominguez, C., Camarero, S., Shleev, S., Polaina, J., Martinez-Arias, A., *et al*. (2008) Combinatorial saturation mutagenesis of the *Myceliophthora thermophila* laccase T2 mutant: the connection between the C-terminal plug and the conserved (509)VSG(511) tripeptide. *Comb Chem High Throughput Screen* **11:** 807–816.

Supporting information

Additional supporting information may be found online in the Supporting Information section at the end of the article.

Fig. S1. Kinetic analysis of recombinant laccases Pp4816 and Pa5930. Pp4816 (A, B, and C) and Pa5930 (D, E, and F) laccases were tested with the substrates ABTS (A, D), ferrocyanide (B, E), and 2,6-DMP (C, F). Oxidation of ABTS and ferrocyanide was followed by registering the OD at 420, and that of 2,6-DMP at 468. Reaction rates were obtained from the linear portion of the progress graph and are plotted against the corresponding substrate concentrations. The kinetic data have been fitted by nonlinear regression to an empirical sigmoid equation, the Hill equation (ABTS, graphs A and D) and to a hyperbolic equation (ferrocyanide and 2,6-DMP, that is B, C, E and F) with the Prism GraphPad program. Kinetic experiments were repeated at least three times with various enzyme concentrations. Only a representative kinetic experiment for each laccase and each substrate, together with resulting fitted substrate-rate curve, is depicted.

Fig. S2. Pa5930 structure at pH 7.5 and 8.5. Superposition of domain 3 in the structures of Pa5930 at Tris-HCl pH 8.5 and HEPES pH 7.5 (in blue hues). The C terminal end of Pa5930 at Tris-HCl pH 8.5 was traced till residue 461 while at HEPES pH 7.5 was traced till residue 471. Structures of domain 3 at Pa5930 (in blue hues) and Pp4816 (in orange) are superposed.

Fig. S3. Structural comparison of Pa5930 and Pp4816 laccases with CotA and CueO. Pa5930 and Pp4816 structures are superposed, and CotA and CueO are shown as individual structures. The three cupredoxin-like domains are color-coded and the long coil region between domain 2 and 3 is colored in red. The Cu ions are also shown in yellow.

Fig. S4. Molecular Phylogenetic analysis by Maximum Likelihood method of LAB laccases from https://lcced.biocatnet.de/. Sequences in the grey zone contain the shorter C terminus, intermediate length in the blue, longer in the green, and longest in the red zone. The evolutionary history was inferred in MEGA7 (S. Kumar, G. Stecher, and K. Tamura, Mol Biol Evol 33:1870-1874, 2016, https://doi.org/10.1093/molbev/msw054) by the Maximum Likelihood method based on the JTT matrixbased model (D.T. Jones, W.R. Taylor, and J.M. Thornton, Comput Appl Biosci 8:275-282, 1992, https://doi.org/10.1093/bioinformatics/8.3.275). Initial trees were obtained by Neighbor-Join and BioNJ algorithms to a matrix of pairwise distances using a JTT model. Branch lengths indicate the number of substitutions per site. The analysis involved 156 sequences and 259 positions, eliminating all gaps and missing data.

Fig. S5. Analysis of the Met rich regions. (A) Superposition of Pa5930 (in blue), Pp4816 (in orange) and CueO (PDB 4E9T, in green) highlighting the C-terminal end of the *Pediococcus* laccases and Met-rich insert at CueO. A sequence alignment between these laccases, including CotA, shows the extension

of C-terminal domain of Pa5930 and Pp4816 and the presence of Met residues (in yellow) and His (in purple). (B) In Pp4816, five Met (designated as an asterisk) at the C-terminal end form a hydrophobic patch at the protein surface.

Fig. S6. Copper coordination site. (A) Superposed Pa5930 (in blue), Pp4816 (in orange), CueO (PDB 4E9T, in green) and CotA (PDB: 3ZDW, in magenta) showing Cu ions (in yellow) and the residues involved in their coordination at CuT1 and TNC site. The cupredoxin-like domains where Cu coordination lies are shown as surface in transparency and color-coded. (B) Superposed Pa5930 and Pp4816 structures showing the Cu ions and residues involved in their coordination at the TNC site together with the acidic residues that surround the TNC site at each laccase.

Fig. S7. The TNC channel. Superposition of Pa5930 (in blue) and Pp4816 (in orange) crystal structures. Waters (modelled as red spheres) leading to the TNC were observed in the Pp4816. The C-terminal extension of Pp4816, distal from the TNC, caps the channel and inserts several residues into it. Meanwhile Pa5930 lacks this C-terminal extension and has a more exposed TNC.

Fig. S8. Comparison of Pa5930 at pH=3.5 and pH=7.5. (A) Structural overview of the Pa5930 pH 3.5 structure. Two molecules (green and dark green) were observed in the asymmetric unit. (B) A benzamidine coordinates the packing of the two copies of Pa5930 by stacking in between Tyr12 of each. Polar bonds between each molecules Asp30 and benzamidine also stabilize the interface. (C) Comparison of the Pa5930 pH 3.5 (green) and Pa5930 pH 7.5 (blue) structure reveal nearly perfect structural alignment.

Fig. S9. Met residues at the conserved substrate binding site. Superposed structures of Pa5930 (in blue), Pp4816 (in pale orange) and CueO (in green, PDB: 4E9T) showing the ABTS binding site as surface in transparency from CotA structure (PDB: 3ZDW). The Met-rich region of CueO lie at the ABTS binding site as well as M347 in Pa5930 or M389 in Pp4816 precluding substrate binding.

Table S1. Root mean square deviations (r.m.s.d.), in Å, for the superposition of laccase structures.

Table S2. Substrates used at pH 3.0 for soaking or co-crystallization with laccase Pa5930.

